

Investigation of the influence of low-frequency harmonic oscillations on deposited metal

Sergii Novykov*

*E. O. Paton Electric Welding Institute of the National Academy of Sciences of Ukraine,
11 Kazymyr Malevych St., UA-03150 Kyiv, Ukraine*

Received 4 May 2022, received in revised form 12 August 2022, accepted 5 September 2022

Abstract

An analysis of current research results shows that specific changes in the deposited metal microstructure are already observed at the periodical impact of 2.5 Hz frequency on it. However, most current research concerns oscillations from the frequency series, which is much higher than 10 Hz, while the oscillation amplitude values are in the range from tens of microns to 2 mm. This circumstance led to the performance of studies on the influence of mechanical harmonic oscillations of the weld pool with a frequency range from 2.5 to 4.5 Hz at the amplitude of 3–7 mm on the weld pool and the HAZ metal. The specimens for investigations were obtained by the GMAW surfacing process in the condition of weld pool oscillations. Treatment of data was conducted by the least squares regression analysis method to plot polynomials.

Key words: weld pool oscillations, deposited metal hardness

1. Introduction

Increasing the technological strength of welded structures is one of the urgent tasks of our time [1–27]. One of the simplest and least expensive methods to solve this task is the application of mechanical oscillations or vibrations of the welding tool or the weld pool. Strength increase is due to the features of the process of weld pool metal solidification under the conditions of periodical impact. To date, it has been possible to determine the main physicochemical and mechanical processes directly influencing the formation of the characteristic microstructure and creating effective models, but there is still no universal theory that accurately enough describes the nature of oscillations influence. Over recent years quite a large number of works [3–26] have been devoted to the investigation of microstructure formation under the conditions of periodic impact. This impact of the generator of oscillations or vibrations is most often imparted to weld pool melt by welding current [4–6], magnetic field [7, 8], laser and electron beam [9–16], as well as the weld pool or tool [17–24]. Here, the respective increase of the degree of deposited metal microstructure dispersivity, compared to samples produced without peri-

odic impact, essentially improves such service properties of the welded joint as-deposited metal hardness [4, 11, 13, 19, 22, 24], wear resistance [5], impact toughness [4, 20, 24], brittle fracture resistance [4], and tensile strength [4, 8, 11, 14, 17, 18, 21, 24]. Proceeding from the analysis of the data of these works, it can be roughly considered that the frequency range in modern studies is usually within 10 Hz [5]–27 kHz [24], that of amplitudes $-6\ \mu\text{m}$ [24] – 0.5–2 mm [8, 15, 22]. However, it was experimentally proved that refinement of the deposited metal microstructure starts already at the frequency of 1.076 Hz at a deposition on carbon steel [25] by MMA and at 1.56 Hz and 2 mm amplitude at a deposition on the nickel-chromium alloy of Inconel 690 type without welding wire by GTAW [26]. Thus, it can be summarized that the general tendency consists in an increase of the frequency of mechanical oscillations up to frequencies much higher than 10 Hz with simultaneous reduction of amplitude from 1–2 mm, that is, the range of frequencies with approximate values of 1–10 Hz and amplitudes from 2 mm and higher remains little studied. A series of experiments with the application of a welding/surfacing generator with vibrational impact on the welding wire of up to 500 Hz frequency and up to 10 mm effective ampli-

*Corresponding author: e-mail address: novykov76@ukr.net

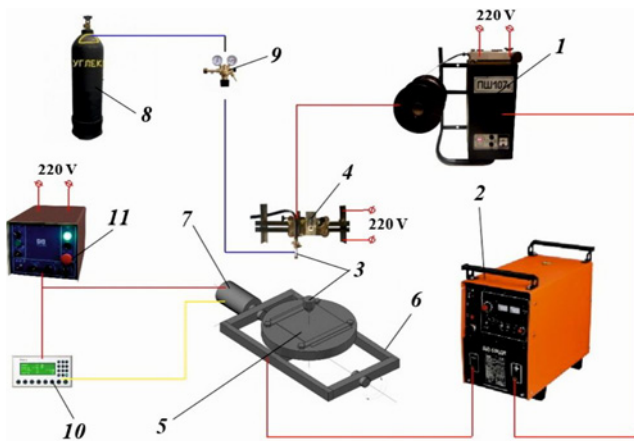


Fig. 1. Overall design diagram of the surfacing installation: 1 – semi-automatic welding machine, 2 – power source, 3 – welding torch, 4 – moving bedplate, 5 – surfaced part, 6 – portable plate, 7 – step motor, 8 – CO₂ cylinder, 9 – gas pressure reducer, 10 – programming panel, 11 – control unit, red – power main, blue – gas main, yellow – main for data input.

tude allowed partially studying the influence of amplitudes of more than 2 mm values [27]. A disadvantage of this device is the high dependence of amplitude on frequency and wire diameter. The most effective oscillation mode was realized at a 2 mm wire diameter. Here, the frequency range was 50–200 Hz, and that of amplitudes was 5–10 mm. Samples produced with the application of this oscillation mode had the deposited metal hardness by 50 HV higher than that of samples produced without an oscillatory impact.

Thus, there is a lack of knowledge about the influence of oscillations of up to 10 Hz frequencies and more than 2 mm amplitudes on the formation of deposited metal microstructure and respective changes of its service properties.

Considering the results of works [8, 25–27], the ranges of frequencies of 2.5–4.5 Hz and amplitudes of 3–7 mm were determined for further studies.

2. Experiment

To conduct experiments on studying the influence of low-frequency oscillations on the weld and HAZ metal, a unit was made on the base of a step motor as a weld pool oscillation source.

The surfacing process was performed by consumable welding wire, fed directly into the weld pool by semi-automatic welding machine 1 (Fig. 1). Welding current of the surfacing process was adjusted by setting the respective rate of welding wire feed by the respective toggle switches, located on the semi-automatic machine control panel. The surfacing current was controlled by appropriate regulators located

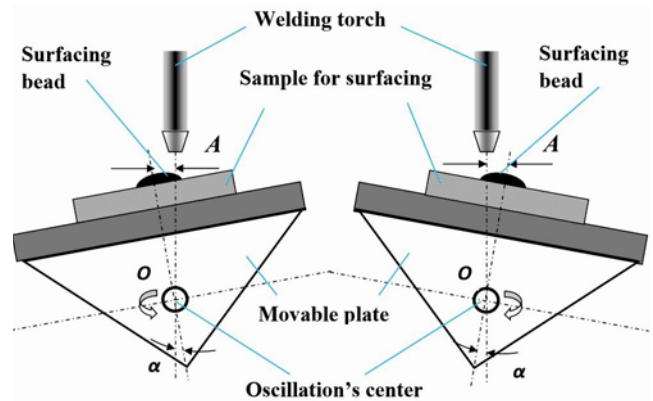


Fig. 2. Principle diagram of a movable plate of traverse oscillations, where A is oscillations amplitude, α is the deviation angle from the surfacing process axis, and O is oscillation's center.

on the face panel of power source 2 due to the indication of the ammeter located there. The open circuit voltage is up to 85 V. Rectilinear movement of welding torch 3 was provided by moving bedplate 4, where the torch was fixed. The surfacing speed was smoothly set by the respective switch on the bedplate control panel. Oscillation of surfaced part 5 was provided by portable table 6, which was movable along a circular arc with a center O to a certain angle α (Fig. 2). The center of this circumference was an axis, which passed the shaft of the step motor 7, which exactly set portable table 6 into motion. The limit value of angle α determined the magnitude of oscillation amplitude A . Active gas is carbon dioxide. It is fed into the arc burning zone from cylinder 8, and its flow rate was set by gas pressure reducer 9.

Batch-produced step motor Kinco 2S86Q-051F6 was selected by a specific procedure by the value of the oscillatory system dynamic moment [28]. Kinco 2M880N driver and Mean Well DRP-240-24 power source were selected in keeping with the values of phase current and supply voltage of the step motor. There are 3 parameters set from the panel: a is the value of angular acceleration in ($\text{rad } \mu\text{s}^{-2}$); imp is the number of micro pulses of motor shaft rotation per cycle; time is the pause time between the micro pulses in (μs). The motor operating parameters were entered from programming panel 10 of Kinco MD 224L grade. Starting the step motor, its stopping, control, programming, and operation mode selection were performed by the respective control unit 11, based on the PLC Kinco-K306-24AT controller.

Oscillation amplitude A was determined to be two times smaller than the oscillation range. It was measured by the value of the trace length, left by a stationary end of the welding wire, touching the part surface at its oscillations. The magnitude of the oscillation

Table 1. Surfacing speed values in oscillation conditions according to Eq. (1)

Starting surfacing speed, V_{ss} (m s^{-1})	Surfacing arc current, I_s (A)	Amplitude of oscillation, A (m)	Frequency of oscillation, ν (Hz)	Width of the bead produced without oscillations, l (m)	Surfacing speed value in oscillation condition, V_{osc} (m s^{-1})	
0.005	100	0.003	3.0	0.006	0.0025	
			4.5		0.0038	
		0.007	3.0		0.0039	
	4.5		0.0059			
	200	0.003	3.0		0.011	0.0032
			4.5			0.0049
0.007		3.0	0.0051			
	4.5	0.0077				

range was regulated by changing the distance from axis O (Fig. 2) to the fastened part surface.

Influence of oscillations on hardness values of deposited metal B and HAZ metal B_{HAZ} was studied as an integral characteristic of mechanical properties, as well as its influence on the microstructure of the deposited and HAZ metal and crystallite size δ . The Vickers hardness test was carried out with a load value of 1 kgF.

The procedure for measuring grain size δ was realized by the random secants method:

1. 5–7 secant lines were drawn in the image of the microstructure of each microsection for the upper, medium, and root parts, respectively. The secant lines were oriented in an arbitrary way relative to each other.

2. The number of intersections of grain boundaries with each secant line was counted.

3. Average grain size is the ratio of the total length of the secant lines for the total number of intersections with grain boundaries.

Investigations were conducted by the least squares procedure of regression analysis [29] by a plan, which was made by the “Latin” squares method [30]. The independent factors are the parameters of the technological mode: arc current I_s , surfacing speed V_s , and those of the oscillation mode: oscillation amplitude A and oscillation frequency ν .

The range of surfacing current values was selected by diameter of 1.2 mm, wire grade ER70S-6 (C: 0.06–0.15 %; Si: 0.80–1.15 %; Mn: 1.40–1.85 %; P: 0.025 %; S: 0.035 %) and type of the surfaced part material (base metal): carbon steel of A568M type. The direction of current arc flow through a welding circuit was DCEP. The surfacing process was carried out by constant current arc welding. This range was as follows (appropriate arc voltage U_s is given in brackets): $I_s = 100$ A ($U_s = 23.5$ V), 125 A ($U_s = 24.7$ V), 150 A

($U_s = 25.8$ V), 175 A ($U_s = 27$ V) and 200 A ($U_s = 28$ V). The applied shield gas was technical 99.5 % CO_2 with a consumption of 9–12 l min^{-1} .

The range of surfacing speed values in oscillation condition V_{osc} was calculated by a dependence, which was determined from the criterion of the deposited bead continuity under the conditions of weld pool oscillations by the following law $y = \frac{L}{2} \sin(2\pi\nu t)$, where $L = 2A$ is the oscillation range and t is the time. The general form of the dependence [31] is as follows:

$$V_{osc} = \pi\nu L \frac{\left(\frac{1}{2n} \left(\frac{l}{L}\right)^2\right) \sqrt{1 - \left(1 - \frac{1}{2n} \left(\frac{l}{L}\right)^2\right)^2}}{\sqrt{\left(\frac{l}{L}\right)^2 - \left(\frac{1}{2n} \left(\frac{l}{L}\right)^2\right)^2}}, \quad (1)$$

where n is the parameter regulating the degree of continuity, the value of which should satisfy the inequality $n > 0.5l/L$, and l is the width of the bead, produced without oscillations at set starting surfacing speed V_{ss} . The limits of value $n = 4.5$ – 6.5 were determined by analysis of this formula, using Mathcad software, and of the features of CO_2 surfacing of 10–12 mm thick samples (Table 1). The established range of surfacing speed value in oscillation condition is $V_{osc} = 0.0025$ – 0.0077 m s^{-1} at frequency $\nu = 3.0, 4.5$ Hz and amplitude $A = 3.0, 7.0$ mm ranges for 1.2 mm wire of ER70S-6 grade at values $l = 0.006$ m and $l = 0.011$ m were obtained by surfacing arc current $I_s = 100$ A and $I_s = 200$ A and starting surfacing speed $V_{ss} = 0.005$ m s^{-1} by $n = 5$.

Thus, the range of V_s values was determined as follows: $V_{osc} = 0.0028, 0.0039, 0.005, 0.0061, \text{ and } 0.0072$ m s^{-1} .

The range of values of oscillation mode parame-

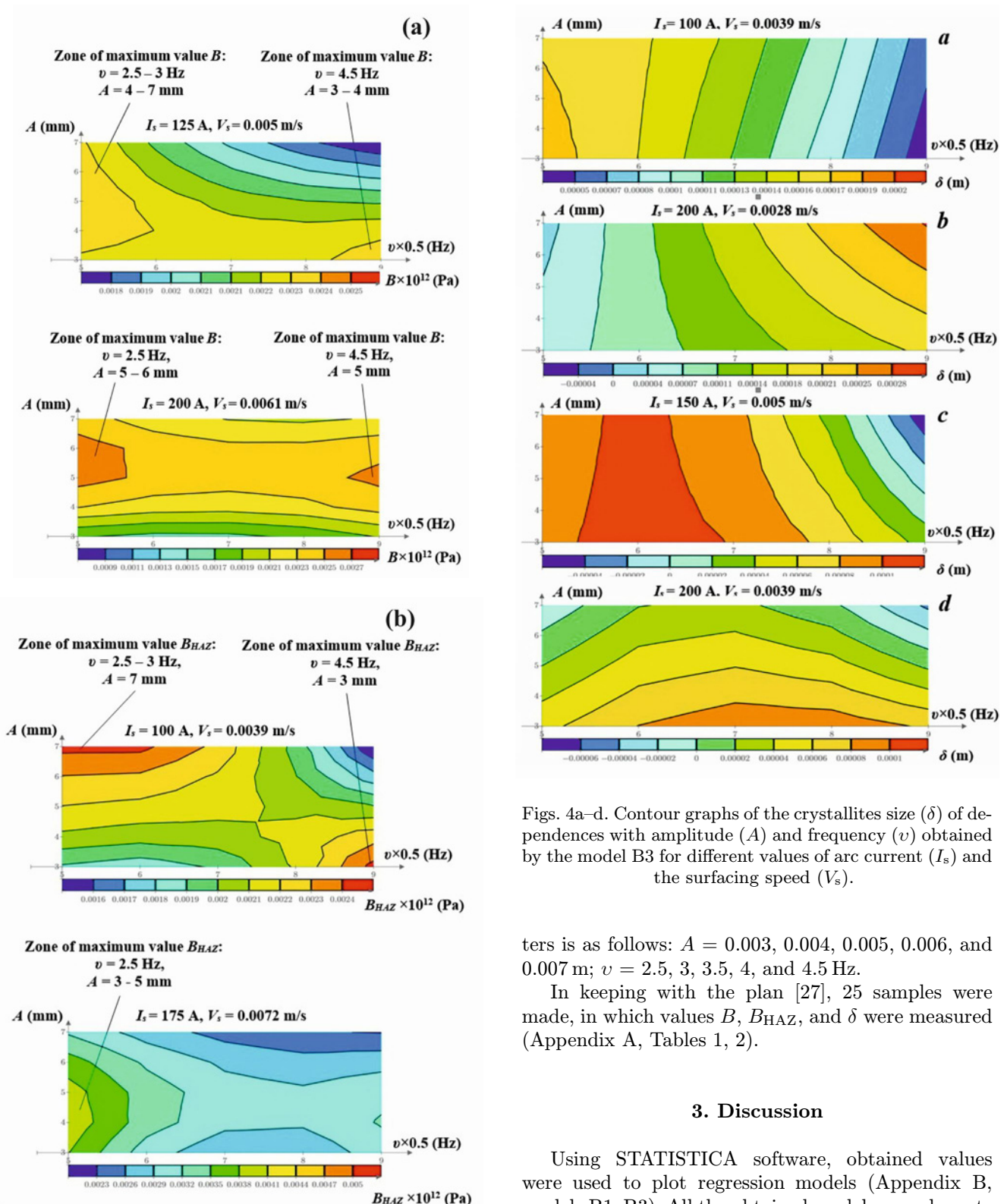


Fig. 3. Characteristic views of contour graphs of dependences of the weld metal hardness (B) and HAZ metal (B_{HAZ}) with amplitude (A) and frequency (v) obtained by the models B1, B2 for different values of arc current (I_s), and the surfacing speed rate (V_s).

Figs. 4a–d. Contour graphs of the crystallites size (δ) of dependences with amplitude (A) and frequency (v) obtained by the model B3 for different values of arc current (I_s) and the surfacing speed (V_s).

ters is as follows: $A = 0.003, 0.004, 0.005, 0.006,$ and 0.007 m; $v = 2.5, 3, 3.5, 4,$ and 4.5 Hz.

In keeping with the plan [27], 25 samples were made, in which values B , B_{HAZ} , and δ were measured (Appendix A, Tables 1, 2).

3. Discussion

Using STATISTICA software, obtained values were used to plot regression models (Appendix B, models B1–B3). All the obtained models are adequate and have degrees of agreement with the true dependence of 85–91%. The models were used to make contour plots, in keeping with which it was established that maximum values B , B_{HAZ} (B1, B2) are most often achieved in the following frequency ranges: $v = 2.5 - 3$ Hz and $v = 4 - 4.5$ Hz (Fig. 3). The ratio of the

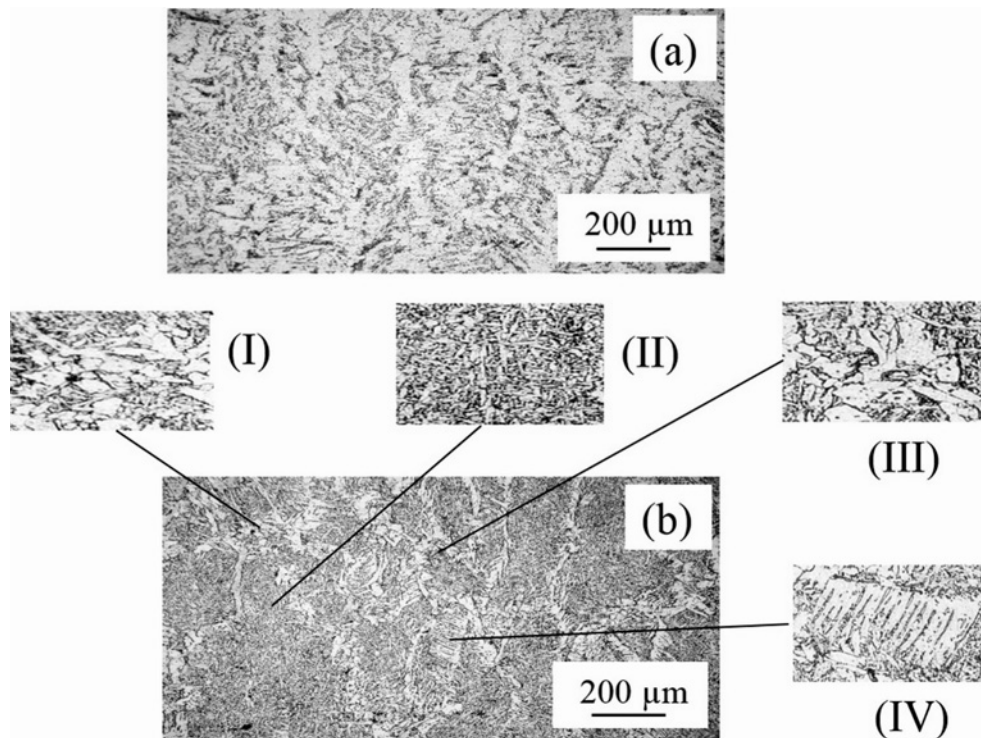


Fig. 5. The microstructure of the weld metal of beads obtained without the influence of oscillations (a) and with the influence of oscillations (b).

factors of current I_s and surfacing speed V_s determines the value of amplitude A and the possibility of formation of the maximum value of hardness in two frequency ranges in one technological mode. Compared to beads produced without oscillations, values B and B_{HAZ} change due to oscillations: value B increases by approximately 7–53%; value B_{HAZ} rises by approximately 27–144%.

The size of the deposited metal crystallite is minimum at frequencies of 2.5–3.5 Hz and 4–4.5 Hz (Figs. 4a,b), depending on the current and surfacing speed ratio, which determines the effective value of amplitude A . Here, the grain size can be reduced a minimum of 1.57 to 2.7 times, but at surfacing with the current of 200 A, the grain size can, contrarily, increase exactly due to oscillations in specific technological modes. Some technological modes can also be used when the grain of minimum size forms at individual frequencies in the entire amplitude range (Fig. 4c) and at individual amplitudes almost in the entire frequency range (Fig. 4d).

In keeping with the obtained data, an optimum surfacing mode was determined by the criteria of minimum value of I_s and a minimum ratio of values B and B_{HAZ} : $I_s = 100$ A, $V_s = 0.0072$ m s⁻¹, $\nu = 2.5$ Hz, $A = 0.007$ m. This mode was used to deposit a bead with the following hardness values: $B = 0.0027$ TPa, $B_{HAZ} = 0.0028$ TPa, which correspond to calculated values within the specified deviations.

The main difference between samples produced

with oscillations and those produced without them consists of greater dispersivity of the microstructure and an increase of the beneficial structural components. Thus, samples produced without the impact of oscillations have the classical ferrite-pearlite structure with relatively wide cast grains, as well as with ferrite interlayers along the cast crystallite boundaries, which are polygonal ferrite precipitates (Fig. 5a by mode $I_s = 100$ A ($U_s = 23.5$ V), $V_s = 0.0028$ m s⁻¹). The influence of oscillations considerably improves the microstructure, and different forms of ferrite are observed (Fig. 5b by mode $I_s = 100$ A ($U_s = 23.5$ V), $V_s = 0.0028$ m s⁻¹, $\nu = 4$ Hz, $A = 0.007$ m): polygonal (Fig. 5b; zone I) – in the form of thin layers along the cast crystallite boundaries; polyhedral (zone III) in the form of individual grains or groups of grains, mostly adjacent to polygonal ferrite; lamellar ferrite with ordered 2nd phase (zone IV), which is carbide precipitation, in the form of parallel rows in the ferrite matrix. Moreover, acicular ferrite (zone II) is observed in the cast crystallite center, as well as small areas of pearlite, which form small dark precipitates adjacent to ferrite grains. Acicular ferrite is accompanied by precipitation of MAC-phase, which also promotes increased hardness and impact toughness. HAZ microstructure is improved owing to the formation of lamellar ferrite and sorbite-like pearlite and an increase in dispersivity degree of them (Fig. 6). Oscillations also promote an essential reduction or complete elimination of such harmful structures as the

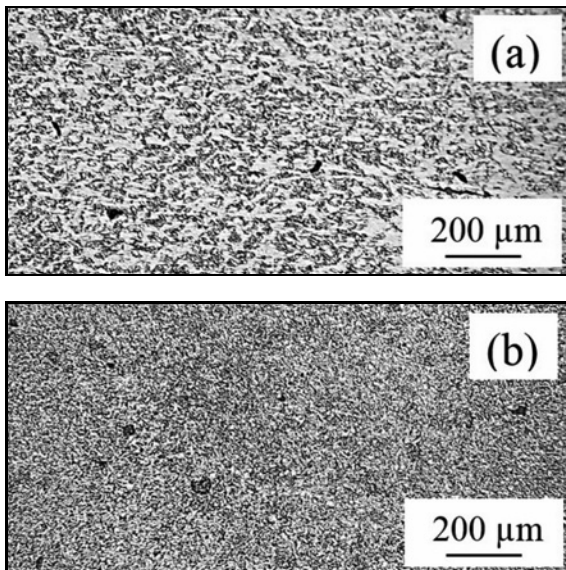


Fig. 6. The microstructure of the HAZ metal of beads obtained without the influence of oscillations (a) and with the influence of oscillations (b).

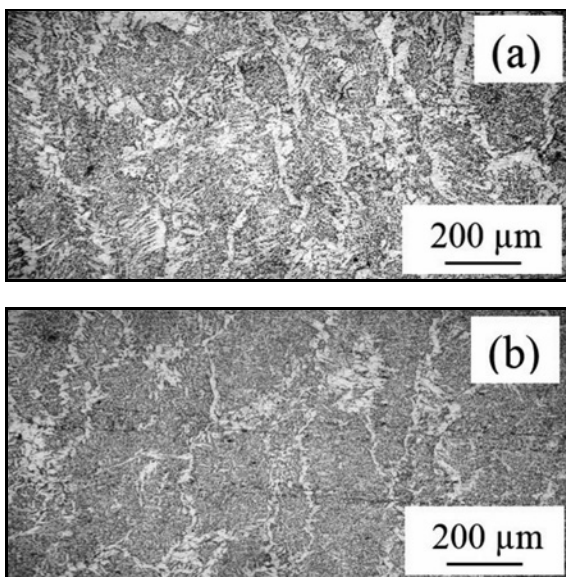


Fig. 7. The microstructure with Widmanstatten structure components of the weld metal of beads obtained without the influence of oscillations (a) and weld metal with the influence of oscillations (b).

Widmanstatten structure (Fig. 7 by mode $I_s = 150$ A ($U_s = 25.8$ V), $V_s = 0.0039$ m s⁻¹, $v = 4$ Hz, and $A = 0.005$ m).

In general, the following overall tendency is observed: better impact on the microstructure occurs at an increase of the technological parameters of the mode, particularly V_s , with an increase of A and simultaneous decrease of v . A better structure, obtained

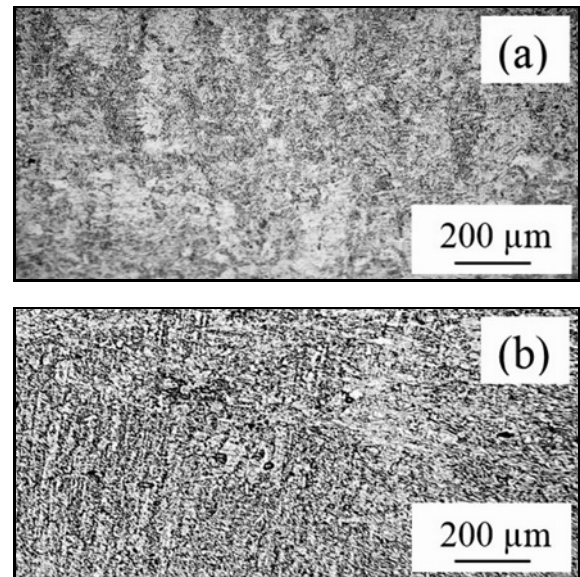


Fig. 8. The microstructure of the weld metal (a) and HAZ metal (b) of beads obtained by mode: $I_s = 125$ A, $V_s = 0.0072$ m s⁻¹, $A = 0.006$ m, and $v = 2.5$ Hz.

using oscillations, is a mixture of upper and lower bainite (Fig. 8) with the martensite-bainite microstructure of the HAZ, which was produced in the following mode: $I_s = 125$ A, $V_s = 0.0072$ m s⁻¹, $A = 0.006$ m, $v = 2.5$ Hz.

Cross-sections of surfaced beads presented are shown in Fig. 9.

4. Conclusions

To increase the hardness of deposited metal and HAZ metal and to ensure a beneficial impact on the deposited metal microstructure, it was proposed to apply mechanical oscillations of the weld pool of up to 4.5 Hz frequency with up to 0.007 m amplitude, using a small-sized model sample of a unit, where a step motor generates the oscillations. The oscillatory mechanism is designed for oscillation of not more than 5 kg mass, and it differs from the available oscillatory mechanisms by simplicity and type of oscillations.

1. On the base of mathematical regression models with the reliability of 85–91 %, plots were obtained of hardness values of dependences of the deposited metal and HAZ metal, and crystallite size, depending on welding arc current, surfacing speed, and oscillation parameters, which showed that compared to surfacing without oscillations, the deposited metal hardness can be increased from 7 to 53 %, that of the HAZ metal – by approximately 27–144 %, and the crystallite size can be reduced 1.57–2.7 times. However, at surfacing with the current of 200 A, the crystallite size will increase exactly due to oscillations.

2. Performed metallographic analysis revealed that

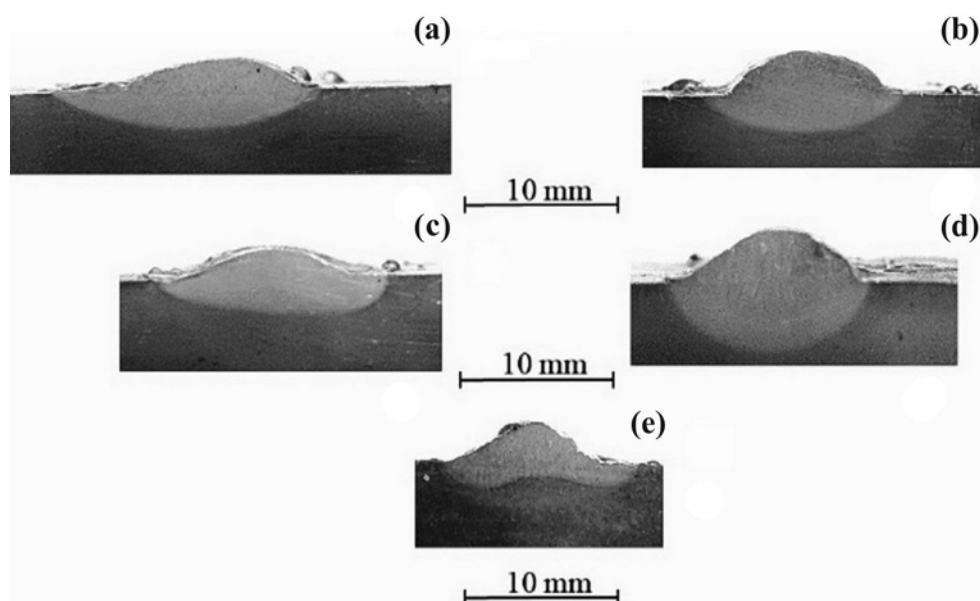


Fig. 9. The general view of cross-sections of surfaced beads obtained by mode $I_s = 100$ A ($U_s = 23.5$ V), $V_s = 0.0028$ m s⁻¹, $v = 4$ Hz, and $A = 0.007$ m: (a) with oscillations influence, (b) without oscillations influence; by mode $I_s = 150$ A ($U_s = 25.8$ V), $V_s = 0.0039$ m s⁻¹, $v = 4$ Hz, and $A = 0.005$ m: (c) with oscillations influence, (d) without oscillations influence, (e) with oscillations influence by mode $I_s = 125$ A, $V_s = 0.0072$ m s⁻¹, $A = 0.006$ m, and $v = 2.5$ Hz.

the main difference between samples produced using oscillations, from those made without them consists not only in an increase of the degree of microstructure refinement but also in an increase of beneficial structural components, such as acicular and lamellar ferrite, which can form not only in the overall microstructure composition but also inside the crystallite body. The HAZ microstructure is improved due to lamellar ferrite and sorbite-like pearlite formation. Application of oscillations allows for reducing or completely avoiding forming harmful structural components, such as the Widmanstätten structure.

3. Based on experimental data processing, the following general tendency was established: mode of surfacing, conducted at higher technological parameters, and, particularly, the surfacing rate, has a better influence on the microstructure; here, an increase of amplitude and simultaneous reduction of frequency are required. A better microstructure is a mixture of upper and lower bainite with martensite-bainite microstructure, providing a maximum hardness value, which is in place at surfacing in the following mode: $I_s = 100$ – 125 A, $V_s = 0.0072$ m s⁻¹, $v = 2.5$ Hz, and $A = 0.006$ – 0.007 m.

References

- [1] J. P. Oliveira, F. M. Braz Fernandes, WP4 Welding and joining techniques for smart materials, Technical Report (2017). <https://doi.org/10.13140/RG.2.2.26647.98725>
- [2] J. Yang, J. P. Oliveira, Y. Li, C. Tan, Ch. Gao, Y. Zhao, Zh. Yu, Laser techniques for dissimilar joining of aluminum alloys to steels: A critical review, *Journal of Materials Processing Technology* 301 (2022) 117443. <https://doi.org/10.1016/j.jmatprotec.2021.117443>
- [3] J. P. Oliveira, J. Shen, Z. Zeng, J. M. Park, Y. T. Choi, N. Schell, E. Maawad, N. Zhou, H. S. Kim, Dissimilar laser welding of a CoCrFeMnNi high entropy alloy to 316 stainless steel, *Scripta Materialia* 206 (2022) 114219. <https://doi.org/10.1016/j.scriptamat.2021.114219>
- [4] A. V. Zavdoveev, V. D. Pozdnyakov, M. Rogante, S. L. Zhdanov, V. A. Kostin, T. G. Solomiychuk, Features of structure formation and properties of joints of S460M steel, made by pulsed-arc welding (in Russian), *Avtomaticheskaya Svarka (Automatic Welding)* 6 (2020) 9–13. <https://doi.org/10.37434/as2020.06.02>
- [5] V. A. Lebedev, I. V. Lendel, A. V. Yarovitsyn, E. I. Los, S. V. Dragan, Peculiarities of formation of structure of welded joints in arc surfacing with pulse feed of electrode wire (in Russian), *Avtomaticheskaya Svarka (Automatic Welding)* 3 (2016) 25–30. <https://doi.org/10.15407/as2016.03.03>
- [6] Yu. N. Saraev, N. I. Golikov, V. V. Dmitriev, I. I. Sannikov, V. P. Bezborodov, A. A. Grigorieva, Investigation of adaptive pulse-arc welding influence on mechanical properties and residual stresses of welded joints in steel grade 09Г2С (in Russian), *Obrabotka Metallov* 3 (2013) 19–24.
- [7] A. D. Razmyshlyaev, M. V. Ageeva, S. A. Bagan, Comparison of the effectiveness of longitudinal and transverse magnetic fields at arc welding and surfacing (in Russian), *Visnyk Donbas'koyi Derzhavnoyi Mashynobudivnoyi Akademiyi* 1 (2019) 55–60.

- [8] V. Subravel, G. Padmanaban, V. Balasubramanian, Optimizing the magnetic arc oscillation process parameters to attain maximum tensile strength using RSM, *Journal of Manufacturing Engineering* 12 (2017) 49–54.
- [9] D. Chai, D. Wu, G. Ma, S. Zhou, Z. Jin, D. Wu, The effects of pulse parameters on weld geometry and microstructure of a pulsed laser welding Ni-base alloy thin sheet with filler wire, *Metals* 6 (2016) 237. <https://doi.org/10.3390/met6100237>
- [10] C. K. Sahoo, S. Mallick, K. Kumar, M. Masanta, Pulse laser welding of high carbon alloy steel: Assessment of melt pool geometry and mechanical performance, *Sādhanā* 46 (2021) 13. <https://doi.org/10.1007/s12046-020-01528-6>
- [11] X. Zhang, L. Li, Y. Chen, Z. Yang, Y. Chen, X. Guo, Effects of pulse parameters on weld microstructure and mechanical properties of extra pulse current aided laser welded 2219 aluminum alloy joints, *Materials* 10 (2017) 109. <https://doi.org/10.3390/ma10091091>
- [12] S. K. Dinda, J. Kar, S. Jana, Effect of beam oscillation on porosity and intermetallics of electron beam welded DP600-steel to Al 5754-alloy, *Journal of Materials Processing Tech.* 265 (2019) 191–200. <https://doi.org/10.1016/j.jmatprotec.2018.10.026>
- [13] T. V. Olshanskaya, G. L. Permyakov, V. Y. Belenkiy, D. N. Trushnikov, The influence of electron beam oscillation on the crystallization and structure of dissimilar steel-bronze welds, *Modern Applied Science* 9 (2015) 296–309. <https://doi.org/10.5539/mas.v9n6p296>
- [14] Z. Tan, B. Pang, J. P. Oliveira, L. Chen, X. Bu, Z. Wang, B. Cong, Z. Zeng, Effect of S-curve laser power for power distribution control on laser oscillating welding of 5A06 aluminum alloy, *Opt. Laser Technol.* 5 (2022) 107909. <https://doi.org/10.1016/j.optlastec.2022.107909>
- [15] W. Ke, X. Bu, J. P. Oliveira, W. Xu, Z. Wang, Z. Zeng, Modeling and numerical study of keyhole-induced porosity formation in laser beam oscillating welding of 5A06 aluminum alloy, *Opt. Laser Technol.* 1 (2021) 106540. <https://doi.org/10.1016/j.optlastec.2020.106540>
- [16] Z. Wang, J. P. Oliveira, Z. Zeng, X. Bu, B. Peng, X. Shao, Laser beam oscillating welding of 5A06 aluminum alloys: Microstructure, porosity and mechanical properties, *Opt. Laser Technol.* 4 (2019) 58–65. <https://doi.org/10.1016/j.optlastec.2018.09.036>
- [17] R. Tamasgavabari, A. Ebrahimi, S. M. Abbasi, A. Yazdipour, Effect of harmonic vibration on microstructure and mechanical properties of AA-5083-H321 aluminum alloy GMAW welds (in Persian), *Journal of Welding Science and Technology of Iran* 5 (2019) 137–149.
- [18] M. V. Rao, P. S. Rao, P. G. Rao, Influence of transverse vibrations on the fatigue life of aluminum alloy weld connections, *International Journal of Mechanical and Production Engineering Research and Development* 10 (2020) 1353–1358. <https://doi.org/10.24247/ijmperdjun2020118>
- [19] C. C. Hsieh, P. S. Wang, J. S. Wang, W. Wu, Evolution of microstructure and residual stress under various vibration modes in 304 stainless steel welds, *The Scientific World Journal* (2014) 895790. <https://doi.org/10.1155/2014/895790>
- [20] J. Kalpana, P. S. Rao, P. G. Rao, Effect of frequency on impact strength of dissimilar weldments produced with vibration, *International Journal of Chemical Sciences* 14 (2016) 1797–1804.
- [21] J. S. Gill, T. K. Reddy, Effect of weld pool vibration on fatigue strength and tensile strength of stainless steel butt welded joints by GTAW process, *Proceedings of The World Congress on Engineering, Vol II WCE* (2018), pp. 721–726. ISBN: 978-988-14048-9-3.
- [22] P. K. Singh, D. Patel, S. B. Prasad, Development of vibratory welding technique and tensile properties investigation of shielded metal arc welded joints, *Indian Journal of Science and Technology* 9 (2016) 1–6. <https://doi.org/10.17485/ijst/2016/v9i35/92846>
- [23] H. Ohrdes, S. Nothdurft, C. Nowroth, J. Grajczak, J. Twiefel, J. Hermsdorf, S. Kaierle, J. Wallaschek, Influence of the ultrasonic vibration amplitude on the melt pool dynamics and the weld shape of laser beam welded EN AW-6082 utilizing a new excitation system for laser beam welding, *Production Engineering* 15 (2021) 151–160. <https://doi.org/10.1007/s11740-020-01008-0>
- [24] H. Chen, N. Guo, K. Xu, C. Liu, G. Wang, Investigating the advantages of ultrasonic-assisted welding technique applied in underwater wet welding by in-situ X-ray imaging method, *Materials* 13 (2020) 1442. <https://doi.org/10.3390/ma13061442>
- [25] V. S. Bade, P. S. Rao, P. G. Rao, Experimental investigation on influence of electrode vibrations on hardness and microstructure of 1018 mild steel weldments, *World Journal of Engineering* 17 (2020) 509–517. <https://doi.org/10.1108/WJE-11-2019-0333>
- [26] A. A. Selvi, Effect of linear direction oscillation on grain refinement. [Master Thesis]. Ohio State University, USA, 2014.
- [27] V. A. Lebedev, I. V. Simutenkov, S. V. Dragan, G. V. Zhuk, S. V. Novykov, Device for automatic surfacing with flux with vibration impact on electrode wires. *Proceedings of Vibration in Engineering and Technology. XVI International Scientific and Technical Conference, Vinnytsia National Technical University* (2017), pp. 71–73.
- [28] V. Lebediev, S. Novykov, Vibrator of product for the automatic arc surfacing. *Tekhnichni nauky ta tekhnolohiyi (Technical sciences and technologies)* 2 (2020) 11–21. [https://doi.org/10.25140/2411-5363-2020-2\(20\)-11-21](https://doi.org/10.25140/2411-5363-2020-2(20)-11-21)
- [29] E. A. Vukolov, *Fundamentals of Statistical Analysis. Workshop on statistical methods and operations research using the STATISTICA and EXEL* (in Russian). Forum, Moscow, 2008. ISBN: 978-5-91134-231-9
- [30] M. M. Protodyakonov, R. I. Teder, *Methodology for Rational Planning of the Experiment* (in Russian), Nauka, Moscow, 1970.
- [31] V. A. Lebedev, S. V. Novikov, Calculation of parameters of automatic arc surfacing of cylindrical details with fluctuating motions of welding instrument, *Blanking productions in mechanical engineering (press forging, foundry and other productions)* 5 (2016) 6–12.

Appendix A

Table 1. The crystallites size value δ in the weld metal of surfacing beads obtained at the appropriate oscillatory (* – without oscillations) and technological modes

Experiment number	I_s (A)	V_s (m s^{-1})	ν (Hz)	A (m)	δ (μm)		
		(in s^{-1})		(in)	Upper part	Medium part	Root part
1*	100	0.0028 0.1102	–	–	258	208	82
1	100	0.0028 0.1102	4	0.007 0.2756	65	113	57
2	100	0.0039 0.1535	3.5	0.006 0.2362	105	108	54
3	100	0.005 0.1969	4.5	0.003 0.1181	90	101	46
4	100	0.0061 0.2402	2.5	0.004 0.1575	25	67	26
5	100	0.0072 0.2835	3	0.005 0.1969	48	58	37
6	125	0.0028 0.1102	3.5	0.003 0.1181	78	90	57
7*	125	0.0039 0.1535	–	–	127	148	46
7	125	0.0039 0.1535	3	0.007 0.2756	67	116	56
8	125	0.005 0.1969	4	0.004 0.1575	69	100	35
9	125	0.0061 0.2402	4.5	0.005 0.1969	114	70	59
10	125	0.0072 0.2835	2.5	0.006 0.2362	-	55	26
11	150	0.0028 0.1102	4.5	0.006 0.2362	117	120	42
12	150	0.0039 0.1535	4	0.005 0.1969	97	132	45
13*	150	0.005 0.1969	–	–	36	113	65
13	150	0.005 0.1969	2.5	0.007 0.2756	36	43	39
14	150	0.0061 0.2402	3	0.003 0.1181	79	159	48
15	150	0.0072 0.2835	3.5	0.004 0.1575	110	79	30
16	175	0.0028 0.1102	3	0.004 0.1575	185	176	64
17	175	0.0039 0.1535	2.5	0.003 0.1181	48.5	52.5	30

Table 1. (continued)

Experiment number	I_s (A)	V_s (m s^{-1})	ν (Hz)	A (m)	δ (μm)		
		(in s^{-1})		(in)	Upper part	Medium part	Root part
18	175	0.005 0.1969	3.5	0.005 0.1969	130	133.5	48.5
19*	175	0.0061 0.2402	–	–	88.6	133	34
19	175	0.0061 0.2402	4	0.006 0.2362	155	130	43
20	175	0.0072 0.2835	4.5	0.007 0.2756	55	77	57
21	200	0.0028 0.1102	2.5	0.005 0.1969	–	174	53.3
22	200	0.0039 0.1535	4.5	0.004 0.1575	60	90	48,3
23	200	0.005 0.1969	3	0.006 0.2362	147	195	47
24	200	0.0061 0.2402	3.5	0.007 0.2756	162	108.3	30
25*	200	0.0072 0.2835	–	–	50	53	24
25	200	0.0072 0.2835	4	0.003 0.1181	109	89	40

Table 2. The hardness of the weld metal B and hardness of HAZ B_{HAZ} values in the weld metal of surfacing beads obtained at the appropriate oscillatory (* – without oscillations) and technological modes

Experiment number	I_s (A)	V_s (m s^{-1})	ν (Hz)	A (m)	$B/B_{\text{HAZ}} \times 10$ (MPa)		
		(in s^{-1})		(in)	Upper part	Medium part	Root part
1*	100	0.0028 0.1102	–	–	163/158	178/162	162/164
1	100	0.0028 0.1102	4	0.007 0.2756	195/217	193/224	187/208
2	100	0.0039 0.1535	3.5	0.006 0.2362	199/212	203/203	203/224
3	100	0.005 0.1969	4.5	0.003 0.1181	217/254	226/261	223/266
4	100	0.0061 0.2402	2.5	0.004 0.1575	223/233	223/229	233/229
5	100	0.0072 0.2835	3	0.005 0.1969	221/217	201/214	210/221
6	125	0.0028 0.1102	3.5	0.003 0.1181	205/208	199/207	217/208
7*	125	0.0039 0.1535	–	–	161/172	167/165	172/175

Table 2. (continued)

Experiment number	I_s (A)	V_s (m s^{-1})	ν (Hz)	A (m)	$B/B_{\text{HAZ}} \times 10$ (MPa)		
		(in s^{-1})		(in)	Upper part	Medium part	Root part
7	125	0.0039 0.1535	3	0.007 0.2756	218/210	219/218	222/214
8	125	0.005 0.1969	4	0.004 0.1575	222/250	224/245	232/248
9	125	0.0061 0.2402	4.5	0.005 0.1969	250/270	232/275	229/272
10	125	0.0072 0.2835	2,5	0.006 0.2362	260/320	279/313	271/317
11	150	0.0028 0.1102	4.5	0.006 0.2362	214/202	214/205	224/205
12	150	0.0039 0.1535	4	0.005 0.1969	229/245	229/243	229/245
13*	150	0.005 0.1969	–	–	205/204	223/197	215/200
13	150	0.005 0.1969	2.5	0.007 0.2756	214/197	210/193	210/195
14	150	0.0061 0.2402	3	0.003 0.1181	222/258	217/260	232/264
15	150	0.0072 0.2835	3.5	0.004 0.1575	251/283	257/287	251/287
16	175	0.0028 0.1102	3	0.004 0.1575	208/220	207/222	203/225
17	175	0.0039 0.1535	2.5	0.003 0.1181	202/173	173/178	178/175
18	175	0.005 0.1969	3.5	0.005 0.1969	208/228	214/228	224/230
19*	175	0.0061 0.2402	–	–	221/197	231/207	214/211
19	175	0.0061 0.2402	4	0.006 0.2362	222/227	219/232	238/229
20	175	0.0072 0.2835	4.5	0.007 0.2756	208/229	219/228	212/229
21	200	0.0028 0.1102	2.5	0.005 0.1969	193/200	193/198	192/203
22	200	0.0039 0.1535	4.5	0.004 0.1575	219/225	225/229	229/229
23	200	0.005 0.1969	3	0.006 0.2362	217/213	226/215	218/214
24	200	0.0061 0.2402	3.5	0.007 0.2756	216/217	214/218	210/219
25*	200	0.0072 0.2835	–	–	193/182	197/184	210/182
25	200	0.0072 0.2835	4	0.003 0.1181	203/215	205/215	179/213

Appendix B

$$\begin{aligned}
 B = & 0.0025115325976854 + 0.0000103364256894232I_s v + \\
 & + 0.0058759267308144I_s V_s + 16.6016450907408AV_s - \\
 & - 0.00241590544247108I_s V_s v + 0.00105829634213171I_s Av - \\
 & - 44.3442907498056AvV_s - 0.000000227768144422142I_s^2 - \\
 & - 106.349123766147V_s^2 - 0.000335306391843706v^2 + \quad (B.1) \\
 & + 41.8181782549147A^2 - 0.00000642951116417346I_s^2 V_s + \\
 & + 0.0000416672416763302I_s^2 A + 0.501025022483833V_s^2 I_s + \\
 & + 0.082027586432854V_s v^2 - 1.4548155487319I_s A^2 + \\
 & + 11490.9078052973AV_s^2 + 7752.10268876331A^3
 \end{aligned}$$

$$\begin{aligned}
 B_{HAZ} = & 0.00138438374248352 + 0.0000047627898806255I_s v + \\
 & + 0.0148950994312386I_s V_s - 0.00590002870031366I_s A + \\
 & + 0.528568771651584Av - 0.723998679511381vV_s - \\
 & - 0.0032205414007356I_s V_s v - 0.178906788144154I_s V_s A + \\
 & + 0.00213983346825101I_s Av - 0.000000156703463044544I_s^2 - \quad (B.2) \\
 & - 0.000024783275040177I_s^2 V_s + 0.0000461175351527008I_s^2 A - \\
 & - 0.131046654276521Av^2 + 0.54718381717974I_s V_s^2 + \\
 & + 0.1607339688102127v^2 V_s - 1.39483213246776I_s A^2 + \\
 & + 8676.57593626603A^3
 \end{aligned}$$

$$\begin{aligned}
 \delta = & 0.00086193978019599 - 0.0000045746854377944I_s - \\
 & - 0.000152825723295094v - 0.099658715277177I_s V_s A + \\
 & + 0.000125847261742664I_s V_s v + 0.0663135721635428I_s V_s^2 + \\
 & + 0.000103968124488349I_s Av^2 - 0.0378703542888321I_s V_s Av^2 + \quad (B.3) \\
 & + 13.5922416750269I_s AvV_s^2 + 0.00000000417935502751238I_s^2 v - \\
 & - 0.000000548232819770337V_s vI_s^2 - 0.00174124657326777V_s v^2 + \\
 & + 2.00770982113061AV_s v^2 + 3.4068932291218vV_s^2 - \\
 & - 0.00593263564907643Av^2 - 3331.1722125233V_s^3
 \end{aligned}$$